ACS APPLIED MATERIALS & INTERFACES

Research Article

www.acsami.org

# Electrochemical Switching with 3D DNA Tetrahedral Nanostructures Self-Assembled at Gold Electrodes

Alireza Abi,[†,‡,§] Meihua Lin,[∥] Hao Pei,[∥] Chunhai Fan,*[,∥] Elena E. Ferapontova,*[,†,‡] and Xiaolei Zuo*[,∥]

[†]Interdisciplinary Nanoscience Center (iNANO), Science and Technology, [‡]Center for DNA Nanotechnology (CDNA) at iNANO, and [§]Sino-Danish Centre for Education and Research (SDC) at iNANO, Aarhus University, Gustav Wieds Vej 1590-14, DK-8000 Aarhus C, Denmark

[∥]Division of Physical Biology, and Bioimaging Center, Shanghai Synchrotron Radiation Facility, CAS Key Laboratory of Interfacial Physics and Technology, Shanghai Institute of Applied Physics, Chinese Academy of Sciences, Shanghai 201800, China

Supporting Information

**ABSTRACT:** Nanomechanical switching of functional three-dimensional (3D) DNA nanostructures is crucial for nanobiotechnological applications such as nanorobotics or self-regulating sensor and actuator devices. Here, DNA tetrahedral nanostructures self-assembled onto gold electrodes were shown to undergo the electronically addressable nanoswitching due to their mechanical reconfiguration upon external chemical stimuli. That enables construction of robust surface-tethered electronic nanodevices based on 3D DNA tetrahedra. One edge of the tetrahedron contained a partially self-complementary region with a stem-loop hairpin structure, reconfigurable upon hybridization to a complementary DNA (stimulus DNA) sequence. A non-intercalative ferrocene (Fc) redox label was attached to the reconfigurable tetrahedron edge in such a way that reconfiguration of this edge changed the distance between the electrode and Fc.

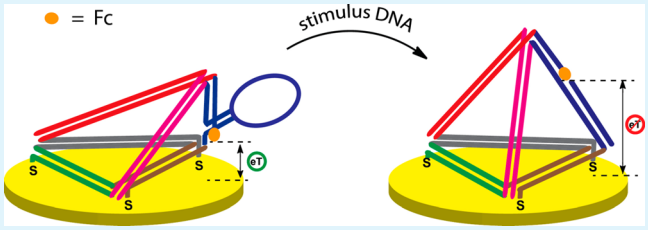


**KEYWORDS:** *DNA nanotechnology, 3D nanostructures, DNA tetrahedron, electromechanical devices, nanomechanical switching, self-assembly*

## INTRODUCTION

High specificity of interactions between DNA bases allows fabrication of two-dimensional (2D) and three-dimensional (3D) nanoscale objects via "bottom-up" DNA self-assembly.[1−3] This way produced DNA nanostructures find numerous applications in the targeted drug delivery,[4,5] metalized DNA nanolithography,[6] fundamental studies of DNA-mediated electron transfer[7] (ET), sensing,[8] and construction of nanomachines, nanoswitchers, and nanomotors, operating as biological sensor and actuator systems.[9−13] Adaptation of such nanomachinery devices for operation at electronically addressable solid supports triggers production of highly efficient and cost effective functional materials with a broad spectrum of activating and sensing properties.[14] Therewith, nanodevice mechanics may be dramatically affected by the properties of conductive supports,[15,16] interfering with the mechanical operation known in solution, and efforts are focused on finding proper strategies for design of robust and functional electronic nanodevices with conserved biorecognition and nanomechanical functions. Here, chemically induced reconfiguration of surface-anchored DNA tetrahedral nanostructures exposed to DNA molecules able to specifically interact with the reconfigurable regions of the tetrahedra was electrochemically interrogated (Figure 1). Developed originally by Turberfield et al.,[17,18] DNA tetrahedron represents a rigid and stable 3D nanostructure formed by self-assembly of four DNA strands. The shape of the tetrahedron can be changed by mechanical reconfiguration of the DNA strand at the edge of the tetrahedron in response to the external stimuli,[19] and such reconfiguration may be exploited for the development of molecular logic gates based on the variation of the Förster resonance energy transfer (FRET) between two fluorophores attached to the opposite sides of the reconfigurable edges.[20] Although configurational transformation of 3D DNA tetrahedral nanostructures has been unambiguously demonstrated in solution, chemically-induced nanomechanical switching of these nanostructures at conductive supports as well as an electronic principle of the event detection have not been established, this being of particular importance for the development of surface-confined stimuli-responsive nanoscale electromechanical devices.

## RESULTS AND DISCUSSION

DNA tetrahedra were assembled by annealing four DNA sequences (the tetrahedron yield of 82%, Table S1 and Figure S2 in the Supporting Information) and then immobilized on the gold surface via thiol linkers at the ends of its three component strands (Figure 1). Immobilization via thiol groups

Received: March 26, 2014
Accepted: May 7, 2014
Published: May 7, 2014

  

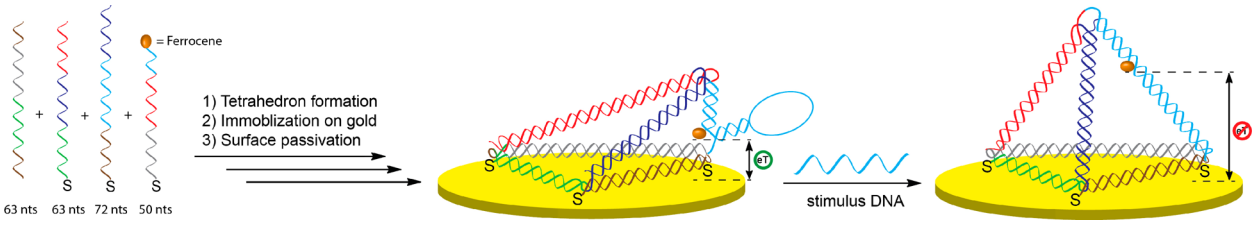


**Figure 1.** Schematic representation of the gold-tethered DNA tetrahedron containing a reconfigurable edge with a stem-loop (hairpin) structure. Reconfiguration of the tetrahedron takes place after hybridization of complementary DNA (stimulus DNA) to the hairpin region, which results in the change of the distance between the Fc redox probe and the electrode surface and thus in the variation of the ferrocene (Fc) electrochemical signal. Mercapto-1-hexanol (MCH) molecules used to block the gold surface are not shown.

was confirmed by quartz crystal microbalance (QCM) studies (Figure S3 in the Supporting Information) and with fluorescently labeled tetrahedra.[21] One of three not parallel to the surface tetrahedron edges contained a partially self-complementary region with a stem-loop hairpin structure, reconfigurable upon hybridization to a complementary DNA sequence. A non-intercalative ferrocene (Fc) redox label was attached to the reconfigurable tetrahedron edge in such a way that reconfiguration of this edge changed the distance between the electrode and Fc. Since the ET efficiency strongly depends on the distance between the redox probe and the electrode,[7,22,23] reconfiguration of the tetrahedron was then probed by monitoring the intensity of the Fc electrochemical signal.

The DNA tetrahedron surface coverage was evaluated by chronocoulometric analysis of the amount of $Ru(NH_3)_6^{3+}$ molecules electrostatically bound to the tetrahedra, according to the previously established protocol.[24] Under the $Ru(NH_3)_6^{3+}$ saturation conditions (Figure S4 in the Supporting Information), the tetrahedron surface coverage was estimated to be 3.2 ± 0.2 pmol $cm^{-2}$ ($n$ = 6), which corresponds to approximately 36% of the theoretical monolayer (8.8 pmol $cm^{-2}$ based on the 7 nm length of the tetrahedron edge).

Since each DNA tetrahedron carries a high sugar-phosphate backbone-associated negative charge resulting from hundreds of DNA bases constituting the tetrahedral structure, the DNA monolayer formed by the immobilized tetrahedra should induce an overall high negative surface charge. Consequently, the electrostatic interactions are expected to play an important role in the accessibility of the tetrahedra binding sites for the reaction with the stimulus molecules, in particular with negatively-charged complementary DNA molecules. In the latter case, the repulsion from the tetrahedron surface layer may prevent their binding to the hairpin regions, and thus will not allow successful reconfiguration resulting in nanomechanical switching of the nanodevice. The extent of the electrostatic repulsion between the tetrahedron-modified electrode surface and negatively charged species was assessed by electrochemical analysis of the $Fe(CN)_6^{4-}/Fe(CN)_6^{3-}$ redox couple bearing essential negative charge. Both electrochemical impedance spectrum (EIS) and cyclic voltammogram (CV) recorded in low ionic strength solution (curve a) evidence that the $Fe(CN)_6^{4-/3-}$ electrochemical reaction is hindered due to the electrostatic repulsion between the redox species and the tetrahedron layer (Figure 2). In higher ionic strength solutions (curves b and c), negative charges of the tetrahedra are effectively compensated by the solution cations and the ET reaction is more efficient due to facilitated diffusion of the redox couple to the electrode surface, with the ET rate constants increasing from 4.1× $10^{-6}$ to 1.4× $10^{-4}$ cm $s^{-1}$ for 10

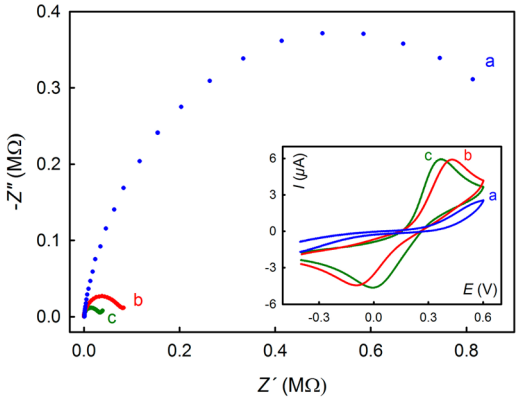


**Figure 2.** Representative EIS recorded with the hybridized tetrahedron-modified gold electrode in the 1 mM $Fe(CN)_6^{3-}$/1 mM $Fe(CN)_6^{4-}$ solution in (a) 10 mM phosphate buffer solution (PBS), (b) 10 mM PBS/0.15 M NaCl, and (c) 10 mM PBS/0.15 M NaCl/10 mM $MgCl_2$. $Z'$ and $-Z''$ are the real and imaginary parts of impedance. Inset: Corresponding CVs, potential scan rate 100 mV $s^{-1}$, other conditions are the same as in the main figure. Lower charge transfer resistance in EIS and less separated CV peaks (curves b,c) are consistent with facilitated diffusion of the redox couple to the electrode surface in the solution of higher ionic strength.

mM PBS and 10 mM PBS containing 0.15 M NaCl/10 mM $MgCl_2$, correspondingly (Table S2 in the Supporting Information). Therefore, high ionic strength conditions seem to be necessary for approaching and reaction of negatively charged molecules (such as DNA) with the tetrahedron binding sites.

Configuration-induced nanomechanical switching of the DNA tetrahedron structures tethered to the electrodes was then electrochemically interrogated in solutions of high ionic strength by following the intensity of the Fc signal. Figure 3 represents the square wave voltammograms (SWV) and corresponding CVs recorded with the tetrahedron-modified electrodes before and after hybridization with complementary DNA, for hybridization conditions see the Supporting Information. Hybridization to complementary DNA resulted in the significantly decreasing Fc current signal, consistent with switching of the tetrahedron configuration from the hairpin closed state to the hybridized extended structure, responsible for the increased distance between the Fc probe and the electrode surface after binding of complementary DNA to the hairpin regions of the tetrahedra. Hybridization of complementary DNA to the surface-tethered tetrahedra was also independently confirmed by the QCM measurements (Figure 4A and the Supporting Information).

It is worth noting that ET between the non-intercalative Fc probe and the electrode does not occur through the DNA


dx.doi.org/10.1021/am501823q | ACS Appl. Mater. Interfaces 2014, 6, 8928−8931

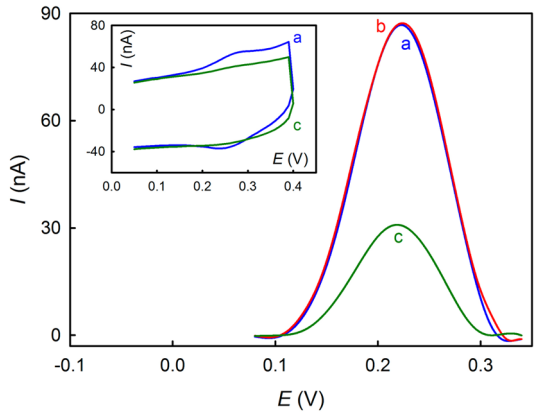


**Figure 3.** Representative baseline-corrected SWVs recorded with the Fc-labeled tetrahedron-modified gold electrode (a) before and (b, c) after reaction with (b) noncomplementary DNA (control) and (c) complementary DNA. SWVs are smoothed (see raw data in Figure S5 in the Supporting Information). Inset: corresponding CVs recorded (a) before and (c) after hybridization with complementary DNA, potential scan rate 100 mV $s^{-1}$. Working solution was 10 mM PBS/0.15 M $NaClO_4$/10 mM $Mg(ClO_4)_2$, pH 7.

duplex (so called DNA-mediated ET),[25] since intercalation into the DNA base stack is necessary for this kind of ET reactions.[16,25] The Fc electrochemistry in the hairpin-tetrahedron state formally followed the diffusion-limited ET kinetics, though with extremely low apparent diffusion rates as can be estimated from the Fc probe diffusion coefficients in the electrode-tethered DNA systems. Those change from $(1.7 \pm 0.4) \times 10^{-6}$ (double stranded dsDNA)[26] to $(8.0 \pm 4) \times 10^{-15}$ $cm^2$ $s^{-1}$ (tetrahedron) and thus in our case are ca. $10^9$ times slower than those observed with dsDNA architectures (Figure S6 and Table S3 in the Supporting Information). Unsurprisingly, the increasing distance between the redox probe and electrode upon tetrahedron reconfiguration substantially decreased the efficiency of ET, which resulted in the diminished Fc signal. Compared to other reported systems,[22,26] relative to its nanoswitching behavior the tetrahedron structure can be thus referred to as one of the most robust electrode-confined architectures hitherto reported.

The efficiency of nanomechanical switching of tetrahedra upon hybridization was estimated by quantification of the extent of hybridization by the $Ru(NH_3)_6^{3+}$ assay.[24] From chronocoulometric responses of the tetrahedron-modified electrodes, before and after hybridization with complementary DNA, approximately 80 ± 12 % ($n$ = 6) of the surface-tethered tetrahedron molecules were estimated to hybridize with complementary DNA thus switching to the hybridized state configuration (Figure 4B and the Supporting Information). Such high efficiency of nanomechanical switching may be ascribed to the rigid tetrahedron nanostructure conserved after immobilization at the electrode surface, lessening the steric hindrance for approaching and binding of stimulus molecules.[21] Additionally, the electrostatic repulsion between the tetrahedron layer and negatively charged molecules diminishes in high ionic strength solutions thus increasing accessibility of the tetrahedron binding sites for complementary DNA molecules. That allowed maintaining dynamic nanoswitching of the electrode surface−attached nanostructures in the most efficient way.

Reconfigurable DNA tetrahedral structures immobilized on electrode surface can be particularly useful for the development of electrochemical biosensors. One of the difficulties nucleic acid−based electrochemical DNA biosensors (particularly those with Fc as the redox label) face is the effect of protein adsorption on the biosensor signal when analysis in complicated biological fluids (e.g., serum) is of interest.[27] The resistance of DNA tetrahedron-modified surfaces against adsorption of serum proteins is an advantage of such surfaces compared to the most of nucleic acid−based sensors and allows quantification of analyte in such complex mixtures.[21,28] Moreover, the very rigid structure of DNA tetrahedron along with its interaction with the surface through three thiols result in highly stable and reproducible electrochemical signals which is beneficial for the development of efficient DNA-based electrochemical biosensors.

## CONCLUSION

Molecular stimulus-induced reconfiguration of DNA tetrahedral nanostructures resulting in the robust electrochemically and chemically controllable nanomechanical switching of the nanostructure was for the first time demonstrated at electrodes. The electrochemical results showed that reconfigurational switching of the surface-confined tetrahedral structures in response to the stimuli DNA molecules takes place with a good efficiency under the high ionic strength condition. That is a first

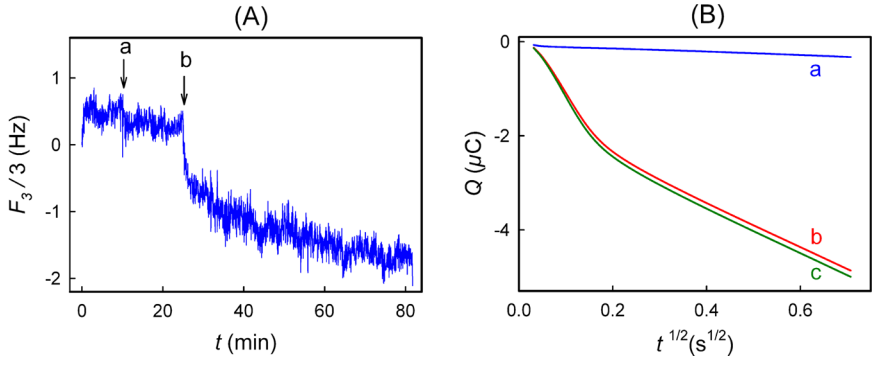


**Figure 4.** (A) Representative QCM spectrum recorded with the tetrahedra-modified gold-plated quartz crystals for consecutive injections of (a) noncomplementary DNA at $t$ = 10 min, and (b) complementary DNA at $t$ = 25 min into the QCM chamber. (B) Representative chronocoulometric responses of the tetrahedron-modified electrode recorded in 10 mM PBS (pH 7.0) containing (a) 0 and (b, c) 0.4 mM $Ru(NH_3)_6^{3+}$, (a,b) before and (c) after hybridization to complementary DNA. Tetrahedron hybridization was performed in high ionic strength solutions (see the Supporting Information).


dx.doi.org/10.1021/am501823q | ACS Appl. Mater. Interfaces 2014, 6, 8928−8931

step in construction of electronically addressable nanoswitching devices based on surface-immobilized 3D DNA architectures.

## ■ ASSOCIATED CONTENT

### Supporting Information

Experimental details: procedures for DNA labeling, tetrahedra assembly, and electrode modification, electrochemical and QCM measurements, estimations of tetrahedra surface coverage and switching efficiency. Tables: DNA sequences; $R_{et}$, $k^0_{et}$, and $D_{eff}$ values. Figures: mass spectra; PAGE analysis; RuHex adsorption isotherm; voltammetric and QCM data. This material is available free of charge via the Internet at http://pubs.acs.org.

## ■ AUTHOR INFORMATION


### Corresponding Authors

*E-mail: fchh@sinap.ac.cn.
*E-mail: elena.ferapontova@inano.au.dk.
*E-mail: zuoxiaolei@sinap.ac.cn.



### Funding

This work was supported by the Sino-Danish Center for Education and Research (SDC) and the Danish National Research Foundation through their support to the Center for DNA Nanotechnology. This work was also supported by the National Natural Science Foundation of China (NSFC, No. 21305151, 21329501) and 100-talent project of Chinese Academy of Sciences.


### Notes

The authors declare no competing financial interest.

## ■ REFERENCES


(1) Rothemund, P. W. K. Folding DNA to Create Nanoscale Shapes and Patterns. *Nature* **2006**, *440*, 297−302.
(2) Andersen, E. S.; Dong, M.; Nielsen, M. M.; Jahn, K.; Subramani, R.; Mamdouh, W.; Golas, M. M.; Sander, B.; Stark, H.; Oliveira, C. L. P.; Pedersen, J. S.; Birkedal, V.; Besenbacher, F.; Gothelf, K. V.; Kjems, J. Self-Assembly of a Nanoscale DNA Box with a Controllable Lid. *Nature* **2009**, *459*, 73−76.
(3) Winfree, E.; Liu, F. R.; Wenzler, L. A.; Seeman, N. C. Design and Self-Assembly of Two-Dimensional DNA Crystals. *Nature* **1998**, *394*, 539−544.
(4) Douglas, S. M.; Bachelet, I.; Church, G. M. A Logic-Gated Nanorobot for Targeted Transport of Molecular Payloads. *Science* **2012**, *335*, 831−834.
(5) Li, J.; Pei, H.; Zhu, B.; Liang, L.; Wei, M.; He, Y.; Chen, N.; Li, D.; Huang, Q.; Fan, C. H. Self-Assembled Multivalent DNA Nanostructures for Noninvasive Intracellular Delivery of Immunostimulatory CpG Oligonucleotides. *ACS Nano* **2011**, *5*, 8783−8789.
(6) Jin, Z.; Sun, W.; Ke, Y.; Shih, C. J.; Paulus, G. L. C.; Wang, Q. H.; Mu, B.; Yin, P.; Strano, M. S. Metallized DNA Nanolithography for Encoding and Transferring Spatial Information for Graphene Patterning. *Nat. Commun.* **2013**, *4*, 1663.
(7) Lu, N.; Pei, H.; Ge, Z. L.; Simmons, C. R.; Yan, H.; Fan, C. H. Charge Transport within a Three-Dimensional DNA Nanostructure Framework. *J. Am. Chem. Soc.* **2012**, *134*, 13148−13151.
(8) Bell, N. A. W.; Engst, C. R.; Ablay, M.; Divitini, G.; Ducati, C.; Liedl, T.; Keyser, U. F. DNA Origami Nanopores. *Nano Lett.* **2012**, *12*, 512−517.
(9) Liu, H.; Liu, D. S. DNA Nanomachines and Their Functional Evolution. *Chem. Commun.* **2009**, 2625−2636.
(10) Yan, H.; Zhang, X. P.; Shen, Z. Y.; Seeman, N. C. A Robust DNA Mechanical Device Controlled by Hybridization Topology. *Nature* **2002**, *415*, 62−65.
(11) Krishnan, Y.; Simmel, F. C. Nucleic Acid Based Molecular Devices. *Angew. Chem., Int. Ed.* **2011**, *50*, 3124−3156.
(12) Ferapontova, E. E.; Mountford, C. P.; Crain, J.; Buck, A. H.; Dickinson, P.; Beattie, J. S.; Ghazal, P.; Terry, J. G.; Walton, A. J.; Mount, A. R. Electrochemical Control of a DNA Holliday Junction Nanoswitch by $Mg^{2+}$ Ions. *Biosens. Bioelectron.* **2008**, *24*, 422−428.
(13) Yang, Y.; Liu, G.; Liu, H. J.; Li, D.; Fan, C. H.; Liu, D. S. An Electrochemically Actuated Reversible DNA Switch. *Nano Lett.* **2010**, *10*, 1393−1397.
(14) Wilner, O. I.; Willner, I. Functionalized DNA Nanostructures. *Chem. Rev.* **2012**, *112*, 2528−2556.
(15) Kaiser, W.; Rant, U. Conformations of End-Tethered DNA Molecules on Gold Surfaces: Influences of Applied Electric Potential, Electrolyte Screening, and Temperature. *J. Am. Chem. Soc.* **2010**, *132*, 7935−7945.
(16) Abi, A.; Ferapontova, E. E. Unmediated by DNA Electron Transfer in Redox-Labeled DNA Duplexes End-Tethered to Gold Electrodes. *J. Am. Chem. Soc.* **2012**, *134*, 14499−14507.
(17) Goodman, R. P.; Berry, R. M.; Turberfield, A. J. The Single-Step Synthesis of a DNA Tetrahedron. *Chem. Commun.* **2004**, 1372−1373.
(18) Goodman, R. P.; Schaap, I. A. T.; Tardin, C. F.; Erben, C. M.; Berry, R. M.; Schmidt, C. F.; Turberfield, A. J. Rapid Chiral Assembly of Rigid DNA Building Blocks for Molecular Nanofabrication. *Science* **2005**, *310*, 1661−1665.
(19) Goodman, R. P.; Heilemann, M.; Doose, S.; Erben, C. M.; Kapanidis, A. N.; Turberfield, A. J. Reconfigurable, Braced, Three-Dimensional DNA Nanostructures. *Nat. Nanotechnol.* **2008**, *3*, 93−96.
(20) Pei, H.; Liang, L.; Yao, G. B.; Li, J.; Huang, Q.; Fan, C. H. Reconfigurable Three-Dimensional DNA Nanostructures for the Construction of Intracellular Logic Sensors. *Angew. Chem., Int. Ed.* **2012**, *51*, 9020−9024.
(21) Pei, H.; Lu, N.; Wen, Y. L.; Song, S. P.; Liu, Y.; Yan, H.; Fan, C. H. A DNA Nanostructure-based Biomolecular Probe Carrier Platform for Electrochemical Biosensing. *Adv. Mater.* **2010**, *22*, 4754−4758.
(22) Fan, C. H.; Plaxco, K. W.; Heeger, A. J. Electrochemical Interrogation of Conformational Changes as a Reagentless Method for the Sequence-Specific Detection of DNA. *Proc. Natl. Acad. Sci. U.S.A.* **2003**, *100*, 9134−9137.
(23) Farjami, E.; Campos, R.; Ferapontova, E. E. Effect of the DNA End of Tethering to Electrodes on Electron Transfer in Methylene Blue-Labeled DNA Duplexes. *Langmuir* **2012**, *28*, 16218−16226.
(24) Steel, A. B.; Herne, T. M.; Tarlov, M. J. Electrochemical Quantitation of DNA Immobilized on Gold. *Anal. Chem.* **1998**, *70*, 4670−4677.
(25) Kelley, S. O.; Jackson, N. M.; Hill, M. G.; Barton, J. K. Long-Range Electron Transfer through DNA Films. *Angew. Chem., Int. Ed.* **1999**, *38*, 941−945.
(26) Anne, A.; Demaille, C. Dynamics of Electron Transport by Elastic Bending of Short DNA Duplexes. Experimental Study and Quantitative Modeling of the Cyclic Voltammetric Behavior of 3′-ferrocenyl DNA End-Grafted on Gold. *J. Am. Chem. Soc.* **2006**, *128*, 542−557.
(27) Ferapontova, E. E.; Gothelf, K. V. Effect of Serum on an RNA Aptamer-Based Electrochemical Sensor for Theophylline. *Langmuir* **2009**, *25*, 4279−4283.
(28) Wen, Y. L.; Pei, H.; Wan, Y.; Su, Y.; Huang, Q.; Song, S. P.; Fan, C. H. DNA Nanostructure-Decorated Surfaces for Enhanced Aptamer-Target Binding and Electrochemical Cocaine Sensors. *Anal. Chem.* **2011**, *83*, 7418−7423.